

# Linear Representations of Hierarchical Concepts in Language Models

Masaki Sakata<sup>1,2</sup>, Benjamin Heinzerling<sup>2,1</sup>, Takumi Ito<sup>1,4</sup>,  
Sho Yokoi<sup>3,1,2</sup>, Kentaro Inui<sup>5,1,2</sup>

<sup>1</sup> Tohoku University   <sup>2</sup> RIKEN   <sup>3</sup> NINJAL   <sup>4</sup> Langsmith Inc.   <sup>5</sup> MBZUAI  
sakata.masaki.s5@dc.tohoku.ac.jp   benjamin.heinzerling@riken.jp  
t-ito@tohoku.ac.jp   yokoi@ninjal.ac.jp   kentaro.inui@mbzuai.ac.ae

## Abstract

We investigate how and to what extent hierarchical relations (e.g., Japan  $\subset$  Eastern Asia  $\subset$  Asia) are encoded in the internal representations of language models. Building on Linear Relational Concepts (Chanin et al., 2024), we train linear transformations specific to each hierarchical depth and semantic domain, and characterize representational differences associated with hierarchical relations by comparing these transformations. Going beyond prior work on the representational geometry of hierarchies in LMs, our analysis covers multi-token entities and cross-layer representations. Across multiple domains we learn such transformations and evaluate in-domain generalization to unseen data and cross-domain transfer. Experiments show that, within a domain, hierarchical relations can be linearly recovered from model representations. We then analyze how hierarchical information is encoded in representation space. We find that it is encoded in a relatively low-dimensional subspace and that this subspace tends to be domain-specific. Our main result is that hierarchy representation is highly similar across these domain-specific subspaces. Overall, we find that all models considered in our experiments encode concept hierarchies in the form of highly interpretable linear representations.

📄: [github.com/masaki-sakata/linear-hierarchical-encoding](https://github.com/masaki-sakata/linear-hierarchical-encoding)

## 1 Introduction

The question if and how language models (LMs) form geometric representations of concepts (Gardenfors, 2004) is of both theoretical (Huh et al., 2024; Coelho Mollo & Millière, 2026) and practical importance (Zou et al., 2023; Templeton et al., 2024; Arditi et al., 2024). Recent work has answered this question positively by identifying geometric representations of concept structures ranging from colors (Abdou et al., 2021) and relational knowledge (Merullo et al., 2024) to geographic location and time (Gurnee & Tegmark, 2024; Heinzerling & Inui, 2024). Most recently, Park et al. (2025) extended this line of research to concept hierarchies, showing that the unembedding layer encodes hierarchical relations geometrically.

However, understanding of how LMs represent hierarchical concepts is still very limited. First, Park et al. (2025) only study static representations in the unembedding layer. Since LMs encode many relations across intermediate layers (Merullo et al., 2024; Hernandez et al., 2024; Chanin et al., 2024), any analysis restricted to a single layer captures only a small part of the model’s representational capacity. Second, Park et al.’s method is limited to concepts that correspond to a single token in the LM’s vocabulary and hence cannot handle hierarchical relations involving multi-token entities, such as *Babe Ruth*  $\subset$  *Baseball Player*.

We address this gap by investigating how LMs represent hierarchies involving diverse, entity-centric concepts across intermediate layers. To this end, we first construct a dataset of concept hierarchies involving multi-token entities, as shown in Fig. 1 (left). We then propose *Linear Hierarchical Encoding* (LHE) as a framework for analyzing cross-layer representations of hierarchies in LMs. We operationalize our framework using Linear Relational Concepts

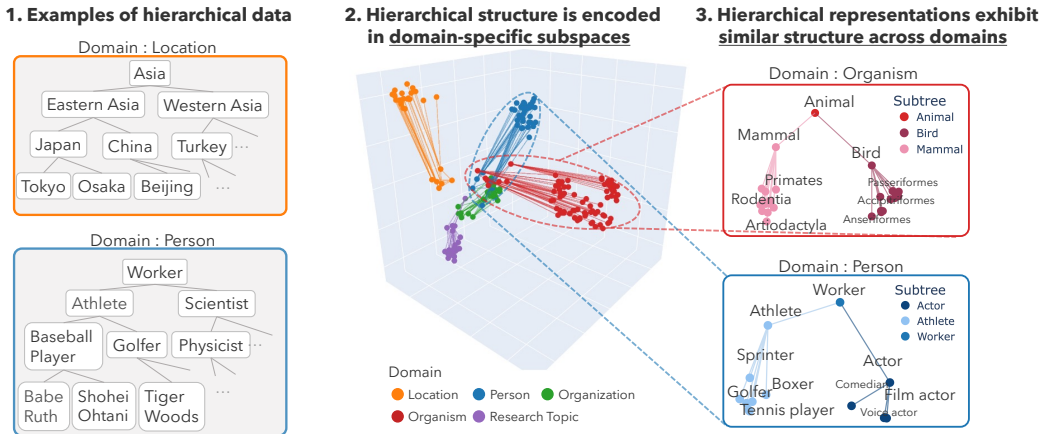


Figure 1: Overview of our main findings. LMs represent hierarchical concepts (left) in domain-specific subspaces of intermediate layer activations (center). The structure of these internal representations is similar across domains (right). The middle and right panels visualize, using PCA, the representations obtained by applying a linear transformation trained on hierarchical data to the hidden-state vectors corresponding to each concept in intermediate layers of Llama 3.1 8B. See App. F for details.

(LRC) (Chanin et al., 2024) to learn depth- and domain-specific linear approximations of the LMs inference process on a hierarchy prediction task (Fig. 2). For example, in the context “Osaka is part of,” we learn a linear transformation that maps an intermediate-layer representation of the child node “Osaka” to the representation of its parent node “Japan”. We train such transformations for each hierarchical depth and domain, and evaluate whether a child node is assigned to the correct parent through the learned transformation.

Empirically, we find that parent–child relations in hierarchies can be linearly recovered from LM representations, and that interventions derived from the learned maps can reliably change the model’s predictions. Further analysis reveals three key properties: (1) hierarchical information is encoded in relatively low-dimensional subspaces, on the order of 150–250 dimensions for models with hidden states size in 3000-5000 range; (2) the relevant subspace is domain-specific; and (3) domain-specific subspaces exhibit a similar hierarchical structure across domains. Taken together, our results show that LMs represent concept hierarchies in a highly interpretable manner.

## 2 Related Work

**Various structures encoded in LMs.** Under the linear representation hypothesis, a growing body of work has shown that LMs encode a wide range of conceptual relations and structures in their internal representations (Abdou et al., 2021; Nanda et al., 2023; Tigges et al., 2023; Burns et al., 2023; Gurnee & Tegmark, 2024; Heinzerling & Inui, 2024; Hernandez et al., 2024; Park et al., 2025). For instance, Abdou et al. (2021) demonstrated that the structure of human color perception is well encoded in LMs. Gurnee & Tegmark (2024) showed that LMs linearly represent spatial and temporal information. These studies suggest that LMs develop internal representations that reflect relational and structural properties of concepts. Among these forms of conceptual structure, we focus on hierarchical structure. Several studies have examined how such hierarchy is encoded in model representation spaces (Park et al., 2025; Costa et al., 2025). For example, Park et al. (2025) showed that hierarchical concepts are represented as approximately orthogonal subspaces in LM unembedding spaces. Compared with these prior studies, our study differs in two important ways. First, on the analysis side, we explicitly examine intermediate-layer representations in LMs and the computations that produce them (Fig. 2). Second, on the data side, we broaden the scope of concepts under study by going beyond single-token words to include more diverse concept sets, such as multi-token entities and class names (Fig. 1, left).

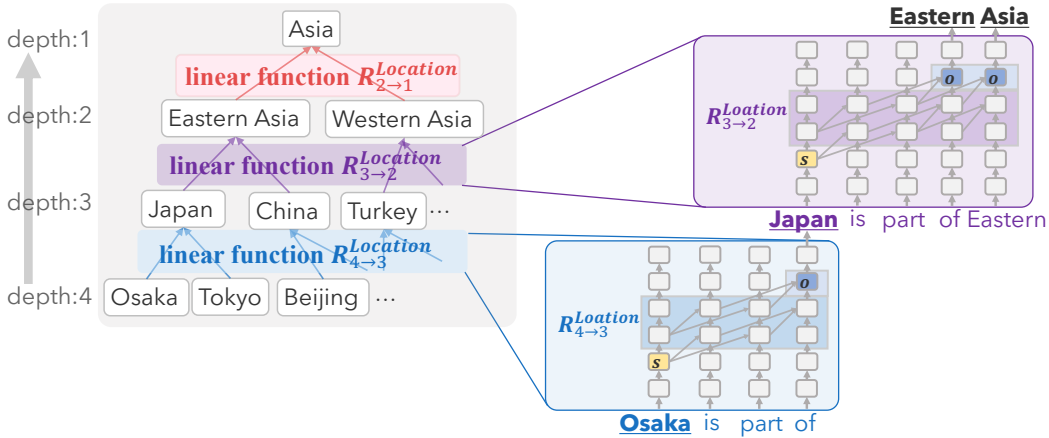


Figure 2: Overview of *Linear Hierarchical Encoding* (LHE). Given a hierarchical relation, LHE learns depth-specific and domain-specific linear transformations that map a child concept representation to the representation of its parent concept in LM intermediate layers.

**Linearity of relation representations in language models.** From a methodological perspective, the work most closely related to ours is that on Linear Relational Embeddings (LRE) in LMs (Hernandez et al., 2024) and Linear Relational Concepts (LRC) (Chanin et al., 2024). LRE considers knowledge represented as subject–relation–object triples, such as (Miles Davis, plays, trumpet), and linearly approximates the computation performed in an LM’s intermediate layers when predicting the object from the subject and relation. It shows that this computation can be approximated reasonably well by a single linear transformation. LRC extends LRE to the multi-token setting and shows that it can identify directions in intermediate-layer representations that correspond to concepts. Our LHE builds on the LRC framework by learning separate models for each hierarchical depth and domain. This allows us to study how hierarchical information is encoded in LM intermediate-layer representations in relation to the computations that produce them.

### 3 Linear Hierarchical Encoding

**From Linear Relation Representations to Linear Hierarchy Representations.** A concept hierarchy consists of relations such as *is-a* and *part-of* that link child concepts to parent concepts. Prior work (Hernandez et al., 2024; Chanin et al., 2024) showed that language models encode such relations linearly: a relation-specific linear map sends the subject representation to the object representation at a later layer. Hierarchies add an additional constraint: the same relation can occur at different depths. For example, an *is-a* relation may connect depth 4 to 3 or depth 3 to 2. We therefore model hierarchy representations with depth-specific linear maps. Concretely, we learn separate transformations for *is-a* at depth  $4 \rightarrow 3$  and at depth  $3 \rightarrow 2$  (Figure 2). This approach allows us to compare maps for the same relation across depths and to test whether they can be exchanged, for example across domains at matched depths, thereby making hierarchical structure directly analyzable.

**Setup.** We represent each instance on a hierarchy  $\mathcal{T}$  as a triple  $(s, r, o)$ , where the subject  $s$  is a child node and the object  $o$  is its parent node. The relation  $r$  is a label indicating a hierarchical transition, and we distinguish  $r$  by depth. For example, in the chain Japan→Eastern Asia→Asia, the transition between depths 2 and 3 is represented as  $(s, r, o) = (\text{Japan}, \text{PART-OF}_{2-3}, \text{Eastern Asia})$ .

**Learning level-wise concept directions.** Following Chanin et al. (2024), we obtain a representation of child node  $s$  by taking the hidden state at layer  $\ell_s$  at the last token position  $i$  of  $s$ , i.e.,  $\mathbf{s}_i = \mathbf{h}_i^{(\ell_s)}$ . For the parent node  $o$ , we define its representation  $\mathbf{o}_n$  as the mean of the hidden states at layer  $\ell_o$  over all tokens constituting  $o$ . For each relation  $r$ , we approximate

Depth	Locations	Research Topic	Persons	Organizations	Organisms
0 (Root)	1	1	1	1	1
1	5	4	6	6	6
2	22	25	35	21	87
3	263	219	224	235	461
4	27971	4464	-	-	-

Table 1: Number of examples by hierarchical depth across domains

the mapping from  $\mathbf{s}$  to  $\mathbf{o}$  using a Linear Relation Embedding (LRE) (Hernandez et al., 2024):

$$R_r(\mathbf{s}) = \mathbf{W}_r \mathbf{s} + \mathbf{b}_r. \quad (1)$$

We estimate  $\mathbf{W}_r$  and  $\mathbf{b}_r$ , where  $\mathbf{W}_r$  is computed as the average Jacobian  $\frac{\partial F}{\partial \mathbf{s}} \Big|_{(s_i, c_i)}$  over samples  $(s_i, c_i)$ , and  $\mathbf{b}_r$  is the corresponding average bias term. Following Chanin et al. (2024), we use a low-rank pseudo-inverse  $\mathbf{W}_r^\dagger$  to define the inverse mapping

$$R_r^\dagger(\mathbf{o}) = \mathbf{W}_r^\dagger(\mathbf{o} - \mathbf{b}_r). \quad (2)$$

and apply this inverse map to obtain a concept vector (concept direction)  $\mathbf{v}_{r,c}$  for each parent concept  $c$ . Intuitively,  $\mathbf{v}_{r,c}$  can be seen as a prototype direction in the child-representation space for nodes with parent concept  $c$ . Let  $\mathcal{I}_{r,c} = \{n \mid o_n = c\}$  be the index set of examples whose parent is  $c$ . We compute

$$\tilde{\mathbf{v}}_{r,c} = \frac{1}{|\mathcal{I}_{r,c}|} \sum_{n \in \mathcal{I}_{r,c}} \mathbf{W}_r^\dagger(\mathbf{o}_n - \mathbf{b}_r), \quad (3)$$

and normalize it as

$$\mathbf{v}_{r,c} = \frac{\tilde{\mathbf{v}}_{r,c}}{\|\tilde{\mathbf{v}}_{r,c}\|_2}. \quad (4)$$

This yields concept vectors  $\mathbf{v}_{r,c}$  corresponding to concepts such as “part-of:Japan” and “part-of:Asia”. For example, the “part-of:Asia” vector serves as a prototype for child-node representations belonging to “Asia”. For each hierarchical relation  $r$ , we compute the set  $\{\mathbf{v}_{r,c}\}_c$  and refer to the collection across relations as *Linear Hierarchical Encoding (LHE)*.

## 4 Experimental Setup

**Data.** To study hierarchical relations in entity-centric concept sets, we use five domain-specific hierarchical datasets spanning locations (Gurnee & Tegmark, 2024; Duncalfe, 2024), persons, organizations (Vrandečić & Krötzsch, 2014), organisms (Park et al., 2025), and research topics (Barrett, 2024). These datasets contain diverse multi-token entities with each node having a single parent. Dataset statistics are reported in Tbl. 1, and concrete examples are provided in Fig. 1 (left) and Fig. 9. See App. A for full details. To focus our analysis on cases where the LM is likely to already possess knowledge of the hierarchical relation, we filter the dataset to instances that the model answers correctly in a few-shot multiple-choice question answering setting. Statistics for the filtered data for each LM are reported in Tbl. 6. We use the same prompt template both for this filtering step and for all experiments; the prompt format is shown in Fig. 10. To measure generalization to subtrees unseen during training, we construct train/test splits by partitioning each domain tree at the root level. For example, in the location domain, we train on subtrees under Europe, the Americas, and Oceania, and evaluate on the subtrees under Asia and Africa.

**Models.** We analyze four decoder-only LMs: Llama 3.2 3B (Meta, 2024), Llama 3.1 8B (Grattafiori et al., 2024), Qwen3 8B, and Qwen3 14B (Yang et al., 2025). The details of each model are summarized in Tbl. 7. For each model, we report results with the hyperparameter setting that gives high Accuracy and Causality scores. The hyperparameter settings for each model are provided in App. C.

Method	Accuracy					Causality				
	Loc.	Topic	Pers.	Org.	Orgm.	Loc.	Topic	Pers.	Org.	Orgm.
Input averaging	0.41	0.29	0.47	0.35	0.44	0.42	0.05	0.10	0.07	0.18
SVM	0.55	0.36	0.63	0.72	0.55	0.58	0.20	0.32	0.35	0.28
LHE	<b>0.68</b>	<b>0.52</b>	<b>0.89</b>	<b>0.93</b>	<b>0.72</b>	<b>0.67</b>	<b>0.35</b>	<b>0.65</b>	<b>0.57</b>	<b>0.57</b>

Table 2: Comparison of LHE and baselines in terms of Accuracy and Causality across domains for Llama 3.1 8B. Scores are averaged across hierarchical levels. Results for all models are reported in Table 10 and scores by depth in Figure 8.

Model	Accuracy (LHE)					Causality (LHE)				
	Loc.	Topic	Pers.	Org.	Orgm.	Loc.	Topic	Pers.	Org.	Orgm.
Llama 3.2 3B	0.76	<b>0.69</b>	<b>0.92</b>	0.96	<b>0.90</b>	0.63	0.14	<b>0.69</b>	<b>0.75</b>	<b>0.65</b>
Llama 3.1 8B	0.70	0.53	0.88	0.96	0.75	<b>0.65</b>	0.12	0.64	0.52	0.53
Qwen3 8B	<b>0.77</b>	0.62	<b>0.92</b>	<b>0.98</b>	0.81	0.55	<b>0.19</b>	0.46	0.52	0.35
Qwen3 14B	0.76	0.58	0.85	0.90	0.80	0.55	0.12	0.25	0.46	0.12

Table 3: Comparison of model performance using LHE in terms of Accuracy and Causality by domain. The results are computed on child-parent examples shared by all four models after LM-based word-prediction filtering. Scores are averaged across hierarchical levels.

**Evaluation.** To evaluate the extent to which hierarchical concepts are encoded in the LM and causally contribute to next-token prediction, we use two metrics: *Accuracy* and *Causality*. High Accuracy indicates that hierarchical information is linearly decodable from the LM’s internal representations. Specifically, we measure accuracy by testing whether internal representations identify which parent node a child node belongs to. Given a test-time child representation  $\mathbf{a}$ , we predict the parent whose concept vector has the largest inner product:

$$\hat{y} = \arg \max_c \mathbf{v}_{r,c} \cdot \mathbf{a}. \quad (5)$$

Accuracy is the proportion of test examples for which  $\hat{y}$  matches the gold parent.

High Causality indicates that the directions obtained from the learned linear transformation are not merely correlational probes but features that make a causal contribution to the LM’s behavior. We measure whether adding and subtracting concept vectors  $\mathbf{v}_{r,c}$  can change the model’s prediction probabilities in the intended direction. For example, given the prompt “Paris is part of”, we edit the hidden state for “Paris” by subtracting “part of: France” and adding “part of: Germany”, and test whether the LM’s next-token prediction flips to “Germany”. Concretely, when changing the original parent  $c$  to a target parent  $c'$ , we intervene on the final-token child representation at every layer as

$$\mathbf{h}_i^{(\ell)} \leftarrow \mathbf{h}_i^{(\ell)} + \beta \|\mathbf{h}_i^{(\ell)}\|_2 (\mathbf{v}_{r,c'} - \mathbf{v}_{r,c}).$$

We deem an intervention successful if, after editing, the predicted probability of  $c'$  exceeds that of  $c$ . For multi-token parent nodes, we evaluate using the minimum token probability over parent tokens, following Chanin et al. (2024). Strong performance on both metrics suggests hierarchical information is not only linearly decodable, but also causally relevant.

## 5 Results

This section investigates the extent to which hierarchical concept structure is encoded in the intermediate layers of LMs. We first empirically examine whether the proposed LHE is an effective method relative to alternative approaches. We then apply LHE to four LMs and investigate the extent to which hierarchical concept structure is encoded in their intermediate layers. Overall, the results provide empirical support for LHE as an analysis method and suggest that hierarchical concept structure is encoded in the intermediate layers of all four LMs, though the extent varies across models.

<b>[Location] Cairo</b>	<b>All correct</b>
Pred: Cairo $\subset$ <span style="background-color: #e0ffe0;">Egypt ✓</span> $\subset$ <span style="background-color: #e0ffe0;">Northern Africa ✓</span> $\subset$ <span style="background-color: #e0ffe0;">Africa ✓</span>	
Gold: Cairo $\subset$ Egypt $\subset$ Northern Africa $\subset$ Africa	
<b>[Person] Lionel Messi</b>	<b>All correct</b>
Pred: Lionel Messi $\subset$ <span style="background-color: #e0ffe0;">Soccer player ✓</span> $\subset$ <span style="background-color: #e0ffe0;">Athlete ✓</span>	
Gold: Lionel Messi $\subset$ Soccer player $\subset$ Athlete	
<b>[Location] Leping</b>	<b>Bottom ✗, Top ✓</b>
Pred: Leping $\subset$ <span style="background-color: #ffe0e0;">India ✗</span> $\not\subset$ <span style="background-color: #e0ffe0;">Eastern Asia ✓</span> $\subset$ <span style="background-color: #e0ffe0;">Asia ✓</span>	
Gold: Leping $\subset$ China $\subset$ Eastern Asia $\subset$ Asia	
<b>[Organism] Dolphin</b>	<b>Bottom ✓, Top ✗</b>
Pred: Dolphin $\subset$ <span style="background-color: #e0ffe0;">Cetacea ✓</span> $\not\subset$ <span style="background-color: #ffe0e0;">Fish ✗</span>	
Gold: Dolphin $\subset$ Cetacea $\subset$ Mammal	
<b>[Organization] The New York Times Company</b>	<b>Bottom ✗, Top ✓</b>
Pred: The New York Times Company $\subset$ <span style="background-color: #ffe0e0;">Consumer goods company ✗</span> $\subset$ <span style="background-color: #e0ffe0;">Company ✓</span>	
Gold: The New York Times Company $\subset$ Media company $\subset$ Company	

Table 4: Examples for accuracy using Llama 3.1 8B. Each row shows an entity and its predicted parent chain (**Pred**) with step-wise correctness (✓/✗) against the gold chain (**Gold**). Correct and incorrect predicted parents are highlighted in green and red, respectively, and  $\subset$  /  $\not\subset$  indicate inclusion vs. non-inclusion relations between consecutive depths. We group cases by whether errors occur earlier vs. later along the evaluated depth sequence; this table shows representative instances of *All correct*, *Bottom ✗, Top ✓*, and *Bottom ✓, Top ✗*. Additional examples are provided in Appendix Table 9.

	Child	Before	Target	After
<b>Success</b>	Silvassa	<span style="background-color: #e0ffe0;">India</span>	Japan	<span style="background-color: #e0ffe0;">Japan</span>
	Hank Aaron	<span style="background-color: #e0ffe0;">Baseball player</span>	Soccer player	<span style="background-color: #e0ffe0;">Soccer player</span>
<b>Failure</b>	LeBron James	<span style="background-color: #e0ffe0;">Basketball player</span>	Tennis player	<span style="background-color: #ffe0e0;">Basketball player</span>

Table 5: Causality success and failure cases obtained with Llama 3.1 8B. **Before**: the LM’s original prediction. **Target**: the intended prediction after intervention. **After**: the actual prediction after adding the concept vector difference.

**Evaluating LHE as an Analysis Method.** If the hierarchical structure of concepts is represented linearly in the intermediate layers of an LM, LHE should be able to capture it. To test this, we compare LHE with alternative methods and examine whether it achieves higher Accuracy and Causality.

To assess the effectiveness of LHE as an analysis method, we use the two baselines: (i) a linear support vector machine (SVM)<sup>1</sup> and (ii) Input Averaging, which uses the mean of child-node vectors associated with a given parent node as the concept vector for that parent<sup>2</sup>. The experimental details are provided in App. B.

Tbl. 2 presents the results. In all domains, LHE achieves higher Accuracy than the baselines. This suggests that the model’s internal representations contain hierarchical information about which parent node each child node belongs to, and that this information can be recovered to a large extent by the linear transformation used in LHE. We observe a similar pattern for Causality. Across all domains, LHE also outperforms the baselines on this metric. Together, the high Accuracy and Causality results indicate that the features captured by the linear transformation are not only useful for recovering hierarchical structure, but also affect the LM’s next-token predictions. Taken together, these results support the use of LHE

<sup>1</sup>Since SVMs cannot naturally predict unseen labels, we include a subset of the test data in training, which makes this a favorable setting for the SVM.

<sup>2</sup>We do not compare to Park et al. (2025)’s method as it is not applicable to intermediate layers.

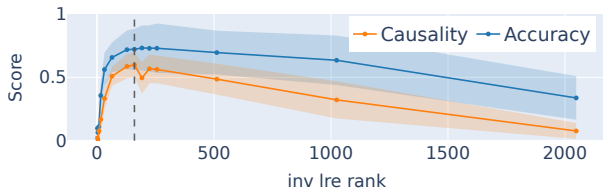


Figure 3: Results of sweeping the rank of the pseudo-inverse matrix  $W_r^\dagger$  for Llama 3.1 8B. Scores are averaged across all domains. The vertical dotted line indicates the point at which the average of Accuracy and Causality is maximized. The results for all models are reported in App. E, confirming that the same trend is consistently observed across models.

as a method for analyzing the hierarchical structure of concepts in the intermediate layers of LMs. Representative success and failure cases are shown in Tables 4 and 5.

**Model Comparison.** Next, we investigate, using LHE, which models encode the hierarchical structure of concepts and to what extent. Tbl. 3 summarizes the results<sup>3</sup>. We find that Accuracy ranges from approximately 0.5 to 0.9 across all models and domains. Causality ranges from 0.35 to 0.7 in most settings, except for the research topic domain and Qwen3 14B. Comparing models, Llama 3.2 3B and Llama 3.1 8B achieve relatively high scores on both Accuracy and Causality, whereas the larger Qwen3 14B model does not achieve the best overall performance. In particular, Qwen3 14B tends to exhibit low Causality. Low Causality indicates that the features extracted by the linear transformation do not substantially contribute to the model’s actual word prediction. This result suggests that, in Qwen3 14B, the representations that influence word prediction may not be linearly encoded.

## 6 Analysis

We analyze how hierarchical structure is encoded in the internal representations of LMs. Specifically, we show that (i) hierarchical information is encoded in a low-dimensional subspace, (ii) the subspace used to encode hierarchical information is largely domain-specific, differing across domains such as locations and persons, and (iii) despite this domain dependence, the structure of hierarchical representations is similar across domains.

**Hierarchy is encoded in a low-dimensional subspace.** We measure the effective rank at which hierarchical information is expressed in the representation space. Concretely, we vary the rank  $k$  of the learned linear operator’s pseudo-inverse  $W_r^\dagger$  and compute both Accuracy and Causality for each setting. Fig. 3 summarizes the results. We find that the scores peak at approximately 150–250 dimensions. This suggests that hierarchical information is concentrated in a relatively low-dimensional subspace.

**Hierarchical structure is encoded in domain-specific subspaces.** Next, we investigate how the encoding of hierarchical structure varies across domains. To this end, we train a linear transformation on one domain and evaluate it on another. Fig. 4 reports the results. Accuracy remains relatively high for many cross-domain combinations, suggesting that the cues needed to linearly recover hierarchical labels are shared to some extent in a domain-general manner. In contrast, Causality is highest within the same domain (the diagonal entries of Fig. 4) and drops substantially under domain shift; for some domain pairs, interventions almost never succeed. This mismatch between the patterns of Accuracy and Causality indicates that being able to decode hierarchical information from representations does not necessarily imply that the features used for decoding are also causally effective for

<sup>3</sup>Note that these results are computed on the intersection of the test instances that remain after word-prediction filtering for all LMs, and thus the test set differs from that used in Tbl. 2.



Figure 4: Cross-domain evaluation of hierarchical-structure directions in Llama 3.1 8B. We train a linear transformation on a domain (x-axis) and evaluate it on test domains (y-axis). Left: Accuracy. Right: Causality (intervention success). Causality drops sharply under domain shift, while Accuracy remains relatively stable. Results for all models in Fig. 12.

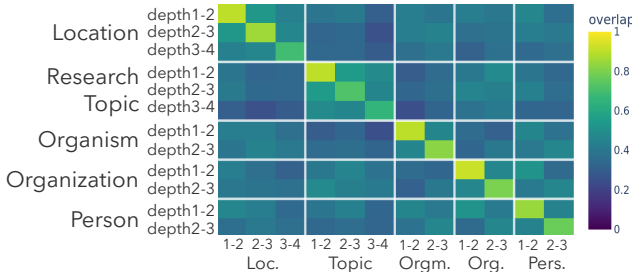


Figure 5: Subspace similarity of subject representations for Llama 3.1 8B. We decompose the learned linear transformation matrix  $W$  via a low-rank SVD,  $W \approx U \text{diag}(s) V^T$ , and quantify the overlap between the subspaces spanned by the right singular vectors  $V$  as  $\text{overlap}(A, B) = \frac{1}{r} \|V_A^T V_B\|_F^2$ , where  $r$  denotes the rank and  $A, B$  are the two conditions being compared. Results for all models in Fig. 16.

prediction. Instead, the intervenable features that affect prediction appear to be encoded differently across domains.

For a more fine-grained analysis, we perform singular value decomposition of the learned linear transformation matrix  $W$  and measure the similarity between the subject-side subspaces involved in causal interventions (Fig. 5). We find that subspace similarity consistently decreases across domains. These results suggest that hierarchical concept representations that causally influence prediction are localized in domain-specific subspaces.

**Hierarchical representations exhibit similar structure across domains.** We now analyze whether the internal representations of hierarchical relations exhibit a shared structure across domains. As a qualitative analysis, we visualize the concept vectors obtained from the learned linear transformations using PCA. Fig. 6 shows that, overall, the vectors form coherent clusters corresponding to subtrees. For example, in the Location domain, vectors associated with concepts under Africa and Asia tend to group together. Moreover, when we apply PCA within each subtree, we observe that the first two principal components often primarily reflect hierarchical depth: vectors at different depths are separated along these components. This suggests a two-level organization in representation space: vectors first cluster by subtree (e.g., Asia), and then encode depth variation within the subtree. We observe similar patterns in other domains (Fig. 6 right, Fig. 1 right, Fig. 17 in App. F), suggesting that the overall representational structure is shared across domains.

To test this hypothesis, we measure the similarity of representational structure using tools from Topological Data Analysis (TDA). TDA enables us to quantify the similarity of structural properties in representations. When there is instance-level correspondence between two point clouds—for example, between sets of hidden-state vectors derived from parallel English–French data—methods such as Representational Similarity Analysis (Kriegeskorte et al., 2008) and Centered Kernel Alignment (Kornblith et al., 2019) are commonly used. In

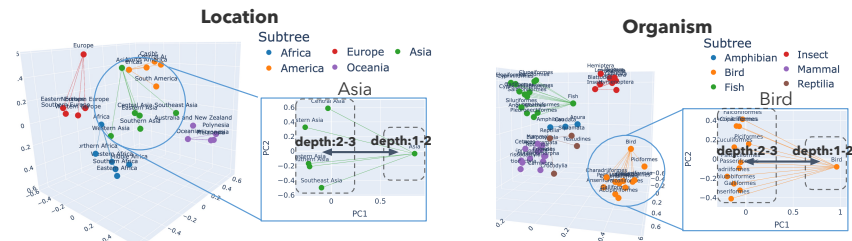


Figure 6: PCA of concept vectors for Llama 3.1 8B in the Location and Organism domains. Concept vectors are obtained by applying a low-rank pseudo-inverse of the learned transformation to parent representations and averaging over examples grouped by parent concept.

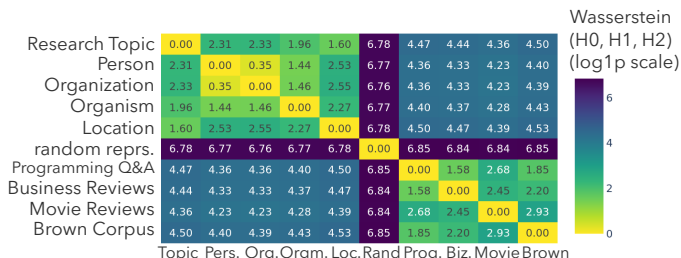


Figure 7: Similarity matrix of LM representations based on persistent homology for Llama 3.1 8B. Each entry shows the Wasserstein distance, computed on persistence diagrams derived from concept vector point clouds, between a pair of domains or datasets. Smaller values indicate more similar representational structure. Results for all models in Fig. 18.

our setting, however, there is no correspondence between individual instances across point clouds. TDA can still be applied in such cases. Implementation details are described in App. G. As baselines, in addition to random representations, we use four non-hierarchical text datasets without hierarchical labels: Programming Q&A (Chandra, 2022), Business Reviews (Zhang et al., 2015), Movie Reviews (Maas et al., 2011), and the Brown Corpus (Kučera & Francis, 1967). We randomly sample nouns from each dataset, extract their LM representations directly from the subject layer, and apply the same TDA procedure. To mitigate biases due to differing sample sizes, we set the baseline sample size to the median of the sample sizes across our hierarchical domains. Fig. 7 reports the resulting Wasserstein-distance matrix. Compared to pairs consisting of a hierarchical domain and a baseline dataset, pairs of hierarchical domains exhibit substantially smaller distances, indicating higher structural similarity. For example, distances between hierarchical-domain pairs are typically in the range 0.3–2.5, whereas distances between a hierarchical domain and a non-hierarchical baseline are around 4.3. Overall, these results support the conclusion that the shape of hierarchical internal representations is broadly similar across domains.

## 7 Conclusion

We analyzed how hierarchical structure is encoded in LM representations using *Linear Hierarchical Encoding* (LHE). Across five domains and four LMs, parent–child relations were linearly recoverable from internal representations, and interventions based on LHE concept directions steered next-token predictions, indicating that extracted features are both decodable and causally relevant. We further found that hierarchical information is encoded in a low-dimensional, largely domain-specific subspace of roughly 150–250 dimensions, while the structure of hierarchical representations is highly similar across domains. These findings suggest that LMs share a domain-general organization for hierarchies, even though the subspace supporting hierarchical encoding is domain-dependent. An interesting direction for future work is to investigate the dynamics of hierarchical representations, including how they emerge during training and how they are modulated in in-context settings.

## Acknowledgments

We would like to thank the members of the Tohoku NLP Group for their insightful comments. This work was supported by JSPS KAKENHI Grant Numbers JP25KJ0628, JP22H05106, JP22H00524, and JP23K24910; JST BOOST Grant Number JPMJBY24F9; and JST FOREST Grant Number JPMJFR2331. This work was supported by ABCI 3.0, which is provided by AIST and AIST Solutions.

## References

- Mostafa Abdou, Artur Kulmizev, Daniel Hershcovich, Stella Frank, Ellie Pavlick, and Anders Søgaard. Can language models encode perceptual structure without grounding? a case study in color. In Arianna Bisazza and Omri Abend (eds.), *Proceedings of the 25th Conference on Computational Natural Language Learning*, pp. 109–132, Online, November 2021. Association for Computational Linguistics. doi: 10.18653/v1/2021.conll-1.9. URL <https://aclanthology.org/2021.conll-1.9/>.
- Andy Arditi, Oscar Obeso, Aaquib Syed, Daniel Paleka, Nina Panickssery, Wes Gurnee, and Neel Nanda. Refusal in language models is mediated by a single direction. *Advances in Neural Information Processing Systems*, 37:136037–136083, 2024.
- Justin Barrett. Openalex topic classification v1 model artifacts and training data, January 2024. URL <https://doi.org/10.5281/zenodo.10568402>.
- Collin Burns, Haotian Ye, Dan Klein, and Jacob Steinhardt. Discovering latent knowledge in language models without supervision. In *The Eleventh International Conference on Learning Representations, ICLR 2023, Kigali, Rwanda, May 1-5, 2023*. OpenReview.net, 2023. URL <https://openreview.net/forum?id=ETKGuby0hcs>.
- Sunny Bhavleen Chandra. stackoverflow-dataset, 2022. URL <https://huggingface.co/datasets/c17hawke/stackoverflow-dataset>. Uploaded by Hugging Face user c17hawke. Accessed 2026-02-21.
- David Chanin, Anthony Hunter, and Oana-Maria Camburu. Identifying linear relational concepts in large language models. In Kevin Duh, Helena Gomez, and Steven Bethard (eds.), *Proceedings of the 2024 Conference of the North American Chapter of the Association for Computational Linguistics: Human Language Technologies (Volume 1: Long Papers)*, pp. 1524–1535, Mexico City, Mexico, June 2024. Association for Computational Linguistics. doi: 10.18653/v1/2024.naacl-long.85. URL <https://aclanthology.org/2024.naacl-long.85/>.
- Dimitri Coelho Mollo and Raphaël Millière. The vector grounding problem. *Philosophy and the Mind Sciences*, 7(1), Feb. 2026. doi: 10.33735/phimisci.2026.12307. URL <https://philosophymindscience.org/index.php/phimisci/article/view/12307>.
- Valérie Costa, Thomas Fel, Ekdeep Singh Lubana, Bahareh Tolooshams, and Demba E. Ba. From flat to hierarchical: Extracting sparse representations with matching pursuit. In *Advances in Neural Information Processing Systems 36 (NeurIPS 2025)*, 2025.
- Luke Duncalfe. ISO-3166-Countries-with-Regional-Codes. <https://github.com/luke/ISO-3166-Countries-with-Regional-Codes/releases/tag/v10.0>, 2024.
- Peter Gardenfors. *Conceptual spaces: The geometry of thought*. MIT press, 2004.
- Aaron Grattafiori, Abhimanyu Dubey, Abhinav Jauhri, Abhinav Pandey, Abhishek Kadian, Ahmad Al-Dahle, Aiesha Letman, Akhil Mathur, Alan Schelten, Alex Vaughan, Amy Yang, Angela Fan, Anirudh Goyal, Anthony Hartshorn, Aobo Yang, Archi Mitra, Archie Sravankumar, Artem Korenev, Arthur Hinsvark, Arun Rao, Aston Zhang, Aurelien Rodriguez, Austen Gregerson, Ava Spataru, Baptiste Roziere, Bethany Biron, Binh Tang, Bobbie Chern, Charlotte Caucheteux, Chaya Nayak, Chloe Bi, Chris Marra, Chris McConnell, Christian Keller, Christophe Touret, Chunyang Wu, Corinne Wong, Cristian Canton Ferrer, Cyrus Nikolaidis, Damien Allonsius, Daniel Song, Danielle Pintz, Danny Livshits, Danny

Wyatt, David Esiobu, Dhruv Choudhary, Dhruv Mahajan, Diego Garcia-Olano, Diego Perino, Dieuwke Hupkes, Egor Lakomkin, Ehab AlBadawy, Elina Lobanova, Emily Dinan, Eric Michael Smith, Filip Radenovic, Francisco Guzmán, Frank Zhang, Gabriel Synnaeve, Gabrielle Lee, Georgia Lewis Anderson, Govind Thattai, Graeme Nail, Gregoire Mialon, Guan Pang, Guillem Cucurell, Hailey Nguyen, Hannah Korevaar, Hu Xu, Hugo Touvron, Iliyan Zarov, Imanol Arrieta Ibarra, Isabel Kloumann, Ishan Misra, Ivan Evtimov, Jack Zhang, Jade Copet, Jaewon Lee, Jan Geffert, Jana Vranes, Jason Park, Jay Mahadeokar, Jeet Shah, Jelmer van der Linde, Jennifer Billock, Jenny Hong, Jenya Lee, Jeremy Fu, Jianfeng Chi, Jianyu Huang, Jiawen Liu, Jie Wang, Jiecao Yu, Joanna Bitton, Joe Spisak, Jongsoo Park, Joseph Rocca, Joshua Johnstun, Joshua Saxe, Junteng Jia, Kalyan Vasuden Alwala, Karthik Prasad, Kartikeya Upasani, Kate Plawiak, Ke Li, Kenneth Heafield, Kevin Stone, Khalid El-Arini, Krithika Iyer, Kshitiz Malik, Kuenley Chiu, Kunal Bhalla, Kushal Lakhotia, Lauren Rantala-Yearly, Laurens van der Maaten, Lawrence Chen, Liang Tan, Liz Jenkins, Louis Martin, Lovish Madaan, Lubo Malo, Lukas Blecher, Lukas Landzaat, Luke de Oliveira, Madeline Muzzi, Mahesh Pasupuleti, Mannat Singh, Manohar Paluri, Marcin Kardas, Maria Tsimpoukelli, Mathew Oldham, Mathieu Rita, Maya Pavlova, Melanie Kambadur, Mike Lewis, Min Si, Mitesh Kumar Singh, Mona Hassan, Naman Goyal, Narjes Torabi, Nikolay Bashlykov, Nikolay Bogoychev, Niladri Chatterji, Ning Zhang, Olivier Duchenne, Onur Çelebi, Patrick Alrassy, Pengchuan Zhang, Pengwei Li, Petar Vasic, Peter Weng, Prajjwal Bhargava, Pratik Dubal, Praveen Krishnan, Punit Singh Koura, Puxin Xu, Qing He, Qingxiao Dong, Ragavan Srinivasan, Raj Ganapathy, Ramon Calderer, Ricardo Silveira Cabral, Robert Stojnic, Roberta Raileanu, Rohan Maheswari, Rohit Girdhar, Rohit Patel, Romain Sauvestre, Ronnie Polidoro, Roshan Sumbaly, Ross Taylor, Ruan Silva, Rui Hou, Rui Wang, Saghar Hosseini, Sahana Chennabasappa, Sanjay Singh, Sean Bell, Seohyun Sonia Kim, Sergey Edunov, Shaoliang Nie, Sharan Narang, Sharath R-parthy, Sheng Shen, Shengye Wan, Shruti Bhosale, Shun Zhang, Simon Vandenhende, Soumya Batra, Spencer Whitman, Sten Sootla, Stephane Collot, Suchin Gururangan, Sydney Borodinsky, Tamar Herman, Tara Fowler, Tarek Sheasha, Thomas Georgiou, Thomas Scialom, Tobias Speckbacher, Todor Mihaylov, Tong Xiao, Ujjwal Karn, Vedanuj Goswami, Vibhor Gupta, Vignesh Ramanathan, Viktor Kerkez, Vincent Gouget, Virginie Do, Vish Vogeti, Vitor Albiero, Vladan Petrovic, Weiwei Chu, Wenhan Xiong, Wenyin Fu, Whitney Meers, Xavier Martinet, Xiaodong Wang, Xiaofang Wang, Xiaoqing Ellen Tan, Xide Xia, Xinfeng Xie, Xuchao Jia, Xuwei Wang, Yaelle Goldschlag, Yashesh Gaur, Yasmine Babaei, Yi Wen, Yiwen Song, Yuchen Zhang, Yue Li, Yuning Mao, Zacharie Delpierre Coudert, Zheng Yan, Zhengxing Chen, Zoe Papakipos, Aaditya Singh, Aayushi Srivastava, Abha Jain, Adam Kelsey, Adam Shajnfeld, Adithya Gangidi, Adolfo Victoria, Ahuva Goldstand, Ajay Menon, Ajay Sharma, Alex Boesenberg, Alexei Baevski, Allie Feinstein, Amanda Kallet, Amit Sangani, Amos Teo, Anam Yunus, Andrei Lupu, Andres Alvarado, Andrew Caples, Andrew Gu, Andrew Ho, Andrew Poulton, Andrew Ryan, Ankit Ramchandani, Annie Dong, Annie Franco, Anuj Goyal, Aparajita Saraf, Arkabandhu Chowdhury, Ashley Gabriel, Ashwin Bharambe, Assaf Eisenman, Azadeh Yazdan, Beau James, Ben Maurer, Benjamin Leonhardi, Bernie Huang, Beth Loyd, Beto De Paola, Bhargavi Paranjape, Bing Liu, Bo Wu, Boyu Ni, Braden Hancock, Bram Wasti, Brandon Spence, Brani Stojkovic, Brian Gamido, Britt Montalvo, Carl Parker, Carly Burton, Catalina Mejia, Ce Liu, Changhan Wang, Changkyu Kim, Chao Zhou, Chester Hu, Ching-Hsiang Chu, Chris Cai, Chris Tindal, Christoph Feichtenhofer, Cynthia Gao, Damon Civin, Dana Beaty, Daniel Kreymer, Daniel Li, David Adkins, David Xu, Davide Testuggine, Delia David, Devi Parikh, Diana Liskovich, Didem Foss, Dingkang Wang, Duc Le, Dustin Holland, Edward Dowling, Eissa Jamil, Elaine Montgomery, Eleonora Presani, Emily Hahn, Emily Wood, Eric-Tuan Le, Erik Brinkman, Esteban Arcaute, Evan Dunbar, Evan Smothers, Fei Sun, Felix Kreuk, Feng Tian, Filippos Kokkinos, Firat Ozgenel, Francesco Caggioni, Frank Kanayet, Frank Seide, Gabriela Medina Florez, Gabriella Schwarz, Gada Badeer, Georgia Swee, Gil Halpern, Grant Herman, Grigory Sizov, Guangyi, Zhang, Guna Lakshminarayanan, Hakan Inan, Hamid Shojanazeri, Han Zou, Hannah Wang, Hanwen Zha, Haroun Habeeb, Harrison Rudolph, Helen Suk, Henry Aspegren, Hunter Goldman, Hongyuan Zhan, Ibrahim Damlaj, Igor Molybog, Igor Tufanov, Ilias Leontiadis, Irina-Elena Veliche, Itai Gat, Jake Weissman, James Geboski, James Kohli, Janice Lam, Japhet Asher, Jean-Baptiste Gaya, Jeff Marcus, Jeff Tang, Jennifer Chan, Jenny Zhen, Jeremy Reizenstein, Jeremy Teboul, Jessica Zhong, Jian Jin, Jingyi Yang, Joe Cummings, Jon Carvill, Jon Shepard, Jonathan

McPhie, Jonathan Torres, Josh Ginsburg, Junjie Wang, Kai Wu, Kam Hou U, Karan Saxena, Kartikay Khandelwal, Katayoun Zand, Kathy Matosich, Kaushik Veeraraghavan, Kelly Michelena, Keqian Li, Kiran Jagadeesh, Kun Huang, Kunal Chawla, Kyle Huang, Lailin Chen, Lakshya Garg, Lavender A, Leandro Silva, Lee Bell, Lei Zhang, Liangpeng Guo, Licheng Yu, Liron Moshkovich, Luca Wehrstedt, Madian Khabsa, Manav Avalani, Manish Bhatt, Martynas Mankus, Matan Hasson, Matthew Lennie, Matthias Reso, Maxim Groshchev, Maxim Naumov, Maya Lathi, Meghan Keneally, Miao Liu, Michael L. Seltzer, Michal Valko, Michelle Restrepo, Mihir Patel, Mik Vyatskov, Mikayel Samvelyan, Mike Clark, Mike Macey, Mike Wang, Miquel Jubert Hermoso, Mo Metanat, Mohammad Rastegari, Munish Bansal, Nandhini Santhanam, Natascha Parks, Natasha White, Navyata Bawa, Nayan Singhal, Nick Egebo, Nicolas Usunier, Nikhil Mehta, Nikolay Pavlovich Laptev, Ning Dong, Norman Cheng, Oleg Chernoguz, Olivia Hart, Omkar Salpekar, Ozlem Kalinli, Parkin Kent, Parth Parekh, Paul Saab, Pavan Balaji, Pedro Rittner, Philip Bontrager, Pierre Roux, Piotr Dollar, Polina Zvyagina, Prashant Ratanchandani, Pritish Yuvraj, Qian Liang, Rachad Alao, Rachel Rodriguez, Rafi Ayub, Raghotham Murthy, Raghu Nayani, Rahul Mitra, Rangaprabhu Parthasarathy, Raymond Li, Rebekkah Hogan, Robin Battey, Rocky Wang, Russ Howes, Ruty Rinott, Sachin Mehta, Sachin Siby, Sai Jayesh Bondu, Samyak Datta, Sara Chugh, Sara Hunt, Sargun Dhillon, Sasha Sidorov, Satadru Pan, Saurabh Mahajan, Saurabh Verma, Seiji Yamamoto, Sharadh Ramaswamy, Shaun Lindsay, Shaun Lindsay, Sheng Feng, Shenghao Lin, Shengxin Cindy Zha, Shishir Patil, Shiva Shankar, Shuqiang Zhang, Shuqiang Zhang, Sinong Wang, Sneha Agarwal, Soji Sajuyigbe, Soumith Chintala, Stephanie Max, Stephen Chen, Steve Kehoe, Steve Satterfield, Sudarshan Govindaprasad, Sumit Gupta, Summer Deng, Sungmin Cho, Sunny Virk, Suraj Subramanian, Sy Choudhury, Sydney Goldman, Tal Remez, Tamar Glaser, Tamara Best, Thilo Koehler, Thomas Robinson, Tianhe Li, Tianjun Zhang, Tim Matthews, Timothy Chou, Tzook Shaked, Varun Vontimitta, Victoria Ajayi, Victoria Montanez, Vijai Mohan, Vinay Satish Kumar, Vishal Mangla, Vlad Ionescu, Vlad Poenaru, Vlad Tiberiu Mihalescu, Vladimir Ivanov, Wei Li, Wenchen Wang, Wenwen Jiang, Wes Bouaziz, Will Constable, Xiaocheng Tang, Xiaojian Wu, Xiaolan Wang, Xilun Wu, Xinbo Gao, Yaniv Kleinman, Yanjun Chen, Ye Hu, Ye Jia, Ye Qi, Yenda Li, Yilin Zhang, Ying Zhang, Yossi Adi, Youngjin Nam, Yu, Wang, Yu Zhao, Yuchen Hao, Yundi Qian, Yunlu Li, Yuzi He, Zach Rait, Zachary DeVito, Zef Rosnbrick, Zhaoduo Wen, Zhenyu Yang, Zhiwei Zhao, and Zhiyu Ma. The llama 3 herd of models, 2024. URL <https://arxiv.org/abs/2407.21783>.

Wes Gurnee and Max Tegmark. Language models represent space and time. In *The Twelfth International Conference on Learning Representations, ICLR 2024, Vienna, Austria, May 7-11, 2024*. OpenReview.net, 2024. URL <https://openreview.net/forum?id=jE8xbmvFin>.

Benjamin Heinzerling and Kentaro Inui. Monotonic representation of numeric attributes in language models. In Lun-Wei Ku, Andre Martins, and Vivek Srikumar (eds.), *Proceedings of the 62nd Annual Meeting of the Association for Computational Linguistics (Volume 2: Short Papers)*, pp. 175–195, Bangkok, Thailand, August 2024. Association for Computational Linguistics. doi: 10.18653/v1/2024.acl-short.18. URL <https://aclanthology.org/2024.acl-short.18/>.

Evan Hernandez, Arnab Sen Sharma, Tal Haklay, Kevin Meng, Martin Wattenberg, Jacob Andreas, Yonatan Belinkov, and David Bau. Linearity of relation decoding in transformer language models. In *The Twelfth International Conference on Learning Representations, ICLR 2024, Vienna, Austria, May 7-11, 2024*. OpenReview.net, 2024. URL <https://openreview.net/forum?id=w7LU2s14kE>.

Minyoung Huh, Brian Cheung, Tongzhou Wang, and Phillip Isola. Position: The platonic representation hypothesis. In *Forty-first International Conference on Machine Learning*, 2024. URL <https://openreview.net/forum?id=BH8TYy0r6u>.

Simon Kornblith, Mohammad Norouzi, Honglak Lee, and Geoffrey E. Hinton. Similarity of neural network representations revisited. In Kamalika Chaudhuri and Ruslan Salakhutdinov (eds.), *Proceedings of the 36th International Conference on Machine Learning, ICML 2019, 9-15 June 2019, Long Beach, California, USA*, Proceedings of Machine Learning Research, pp. 3519–3529. PMLR, 2019. URL <http://proceedings.mlr.press/v97/kornblith19a.html>.

- Nikolaus Kriegeskorte, Marieke Mur, and Peter Bandettini. Representational similarity analysis - connecting the branches of systems neuroscience. *Frontiers in Systems Neuroscience*, 2, 2008. ISSN 1662-5137. doi: 10.3389/neuro.06.004.2008. URL <https://www.frontiersin.org/articles/10.3389/neuro.06.004.2008>.
- Henry Kučera and W. Nelson Francis. *Computational Analysis of Present-Day American English*. Brown University Press, Providence, RI, 1967.
- Andrew L. Maas, Raymond E. Daly, Peter T. Pham, Dan Huang, Andrew Y. Ng, and Christopher Potts. Learning word vectors for sentiment analysis. In *Proceedings of the 49th Annual Meeting of the Association for Computational Linguistics: Human Language Technologies*, pp. 142–150, Portland, Oregon, USA, June 2011. Association for Computational Linguistics. URL <http://www.aclweb.org/anthology/P11-1015>.
- Jack Merullo, Carsten Eickhoff, and Ellie Pavlick. Language models implement simple Word2Vec-style vector arithmetic. In Kevin Duh, Helena Gomez, and Steven Bethard (eds.), *Proceedings of the 2024 Conference of the North American Chapter of the Association for Computational Linguistics: Human Language Technologies (Volume 1: Long Papers)*, pp. 5030–5047, Mexico City, Mexico, June 2024. Association for Computational Linguistics. doi: 10.18653/v1/2024.naacl-long.281. URL <https://aclanthology.org/2024.naacl-long.281/>.
- Meta. Llama 3.2 model card. [https://github.com/meta-llama/llama-models/blob/main/models/llama3\\_2/MODEL\\_CARD.md](https://github.com/meta-llama/llama-models/blob/main/models/llama3_2/MODEL_CARD.md), 2024. Official model card.
- Neel Nanda, Andrew Lee, and Martin Wattenberg. Emergent linear representations in world models of self-supervised sequence models. In Yonatan Belinkov, Sophie Hao, Jaap Jumelet, Najoung Kim, Arya McCarthy, and Hosein Mohebbi (eds.), *Proceedings of the 6th BlackboxNLP Workshop: Analyzing and Interpreting Neural Networks for NLP*, pp. 16–30, Singapore, December 2023. Association for Computational Linguistics. doi: 10.18653/v1/2023.blackboxnlp-1.2. URL <https://aclanthology.org/2023.blackboxnlp-1.2/>.
- Kiho Park, Yo Joong Choe, Yibo Jiang, and Victor Veitch. The geometry of categorical and hierarchical concepts in large language models. In *The Thirteenth International Conference on Learning Representations, ICLR 2025, Singapore, April 24-28, 2025*. OpenReview.net, 2025. URL <https://openreview.net/forum?id=bVTM2QKYuA>.
- Aaditya Singh, Adam Fry, Adam Perelman, Adam Tart, Adi Ganesh, Ahmed El-Kishky, Aidan McLaughlin, Aiden Low, AJ Ostrow, Akhila Ananthram, Akshay Nathan, Alan Luo, Alec Helyar, Aleksander Madry, Aleksandr Efremov, Aleksandra Spyra, Alex Baker-Whitcomb, Alex Beutel, Alex Karpenko, Alex Makelov, Alex Neitz, Alex Wei, Alexandra Barr, Alexandre Kirchmeyer, Alexey Ivanov, Alexi Christakis, Alistair Gillespie, Allison Tam, Ally Bennett, Alvin Wan, Alyssa Huang, Amy McDonald Sandjideh, Amy Yang, Ananya Kumar, Andre Saraiva, Andrea Vallone, Andrei Gheorghe, Andres Garcia Garcia, Andrew Braunstein, Andrew Liu, Andrew Schmidt, Andrey Mereskin, Andrey Mishchenko, Andy Applebaum, Andy Rogerson, Ann Rajan, Annie Wei, Anoop Kotha, Anubha Srivastava, Anushree Agrawal, Arun Vijayvergiya, Ashley Tyra, Ashvin Nair, Avi Nayak, Ben Eggers, Bessie Ji, Beth Hoover, Bill Chen, Blair Chen, Boaz Barak, Borys Minaiev, Botao Hao, Bowen Baker, Brad Lightcap, Brandon McKinzie, Brandon Wang, Brendan Quinn, Brian Fioca, Brian Hsu, Brian Yang, Brian Yu, Brian Zhang, Brittany Brenner, Callie Riggins Zetino, Cameron Raymond, Camillo Lugaresi, Carolina Paz, Cary Hudson, Cedric Whitney, Chak Li, Charles Chen, Charlotte Cole, Chelsea Voss, Chen Ding, Chen Shen, Chengdu Huang, Chris Colby, Chris Hallacy, Chris Koch, Chris Lu, Christina Kaplan, Christina Kim, CJ Minott-Henriques, Cliff Frey, Cody Yu, Coley Czarnecki, Colin Reid, Colin Wei, Cory Decareaux, Cristina Scheau, Cyril Zhang, Cyrus Forbes, Da Tang, Dakota Goldberg, Dan Roberts, Dana Palmie, Daniel Kappler, Daniel Levine, Daniel Wright, Dave Leo, David Lin, David Robinson, Declan Grabb, Derek Chen, Derek Lim, Derek Salama, Dibya Bhattacharjee, Dimitris Tsipras, Dinghua Li, Dingli Yu, DJ Strouse, Drew Williams, Dylan Hunn, Ed Bayes, Edwin Arbus, Ekin Akyurek, Elaine Ya Le, Elana Widmann, Eli Yani, Elizabeth Proehl, Enis Sert, Enoch Cheung, Eri Schwartz, Eric Han, Eric Jiang, Eric Mitchell, Eric Sigler, Eric Wallace, Erik Ritter, Erin Kavanaugh, Evan Mays, Evgenii Nikishin, Fangyuan Li, Felipe Petroski Such, Filipe de Avila Belbute Peres,

Filippo Raso, Florent Bekerman, Foivos Tsimpourlas, Fotis Chantzis, Francis Song, Francis Zhang, Gaby Raila, Garrett McGrath, Gary Briggs, Gary Yang, Giambattista Parascandolo, Gildas Chabot, Grace Kim, Grace Zhao, Gregory Valiant, Guillaume Leclerc, Hadi Salman, Hanson Wang, Hao Sheng, Haoming Jiang, Haoyu Wang, Haozhun Jin, Harshit Sikchi, Heather Schmidt, Henry Aspegren, Honglin Chen, Huida Qiu, Hunter Lightman, Ian Covert, Ian Kivlichan, Ian Silber, Ian Sohl, Ibrahim Hammoud, Ignasi Clavera, Ikai Lan, Ilge Akkaya, Ilya Kostrikov, Irina Kofman, Isak Etinger, Ishaan Singal, Jackie Hehir, Jacob Huh, Jacqueline Pan, Jake Wilczynski, Jakub Pachocki, James Lee, James Quinn, Jamie Kiros, Janvi Kalra, Jasmyn Samaroo, Jason Wang, Jason Wolfe, Jay Chen, Jay Wang, Jean Harb, Jeffrey Han, Jeffrey Wang, Jennifer Zhao, Jeremy Chen, Jerene Yang, Jerry Tworek, Jesse Chand, Jessica Landon, Jessica Liang, Ji Lin, Jiancheng Liu, Jianfeng Wang, Jie Tang, Jihan Yin, Joanne Jang, Joel Morris, Joey Flynn, Johannes Ferstad, Johannes Heidecke, John Fishbein, John Hallman, Jonah Grant, Jonathan Chien, Jonathan Gordon, Jongsoo Park, Jordan Liss, Jos Kraaijeveld, Joseph Guay, Joseph Mo, Josh Lawson, Josh McGrath, Joshua Vendrow, Joy Jiao, Julian Lee, Julie Steele, Julie Wang, Junhua Mao, Kai Chen, Kai Hayashi, Kai Xiao, Kamyar Salahi, Kan Wu, Karan Sekhri, Karan Sharma, Karan Singhal, Karen Li, Kenny Nguyen, Keren Gu-Lemberg, Kevin King, Kevin Liu, Kevin Stone, Kevin Yu, Kristen Ying, Kristian Georgiev, Kristie Lim, Kushal Tirumala, Kyle Miller, Lama Ahmad, Larry Lv, Laura Clare, Laurance Fauconnet, Lauren Itow, Lauren Yang, Laurentia Romaniuk, Leah Anise, Lee Byron, Leher Pathak, Leon Maksin, Leyan Lo, Leyton Ho, Li Jing, Liang Wu, Liang Xiong, Lien Mamitsuka, Lin Yang, Lindsay McCallum, Lindsey Held, Liz Bourgeois, Logan Engstrom, Lorenz Kuhn, Louis Feuvrier, Lu Zhang, Lucas Switzer, Lukas Kondraciuk, Lukasz Kaiser, Manas Joglekar, Mandeep Singh, Mandip Shah, Manuka Stratta, Marcus Williams, Mark Chen, Mark Sun, Marselus Cayton, Martin Li, Marvin Zhang, Marwan Aljubeh, Matt Nichols, Matthew Haines, Max Schwarzer, Mayank Gupta, Meghan Shah, Melody Huang, Meng Dong, Mengqing Wang, Mia Glaese, Micah Carroll, Michael Lampe, Michael Malek, Michael Sharman, Michael Zhang, Michele Wang, Michelle Pokrass, Mihai Florian, Mikhail Pavlov, Miles Wang, Ming Chen, Mingxuan Wang, Minnia Feng, Mo Bavarian, Molly Lin, Moose Abdool, Mostafa Rohaninejad, Nacho Soto, Natalie Staudacher, Natan LaFontaine, Nathan Marwell, Nelson Liu, Nick Preston, Nick Turley, Nicklas Ansmann, Nicole Blades, Nikil Pancha, Nikita Mikhaylin, Niko Felix, Nikunj Handa, Nishant Rai, Nitish Keskar, Noam Brown, Ofir Nachum, Oleg Boiko, Oleg Murk, Olivia Watkins, Oona Gleeson, Pamela Mishkin, Patryk Lesiewicz, Paul Baltescu, Pavel Belov, Peter Zhokhov, Philip Pronin, Phillip Guo, Phoebe Thacker, Qi Liu, Qiming Yuan, Qinghua Liu, Rachel Dias, Rachel Puckett, Rahul Arora, Ravi Teja Mullapudi, Raz Gaon, Reah Miyara, Rennie Song, Rishabh Aggarwal, RJ Marsan, Robel Yemiru, Robert Xiong, Rohan Kshirsagar, Rohan Nuttall, Roman Tsiupa, Ronen Eldan, Rose Wang, Roshan James, Roy Ziv, Rui Shu, Ruslan Nigmatullin, Saachi Jain, Saam Talaie, Sam Altman, Sam Arnesen, Sam Toizer, Sam Toyer, Samuel Miserendino, Sandhini Agarwal, Sarah Yoo, Savannah Heon, Scott Ethersmith, Sean Grove, Sean Taylor, Sebastien Bubeck, Sever Banesiu, Shaokyi Amdo, Shengjia Zhao, Sherwin Wu, Shibani Santurkar, Shiyu Zhao, Shraman Ray Chaudhuri, Shreyas Krishnaswamy, Shuaiqi, Xia, Shuyang Cheng, Shyamal Anadkat, Simón Posada Fishman, Simon Tobin, Siyuan Fu, Somay Jain, Song Mei, Sonya Egoian, Spencer Kim, Spug Golden, SQ Mah, Steph Lin, Stephen Imm, Steve Sharpe, Steve Yadlowsky, Sulman Choudhry, Sungwon Eum, Suvansh Sanjeev, Tabarak Khan, Tal Stramer, Tao Wang, Tao Xin, Tarun Gogineni, Taya Christianson, Ted Sanders, Tejal Patwardhan, Thomas Degry, Thomas Shadwell, Tianfu Fu, Tianshi Gao, Timur Garipov, Tina Sriskandarajah, Toki Sherbakov, Tomer Kaftan, Tomo Hiratsuka, Tongzhou Wang, Tony Song, Tony Zhao, Troy Peterson, Val Kharitonov, Victoria Chernova, Vineet Kosaraju, Vishal Kuo, Vitchyr Pong, Vivek Verma, Vlad Petrov, Wanning Jiang, Weixing Zhang, Wenda Zhou, Wenlei Xie, Wenting Zhan, Wes McCabe, Will DePue, Will Ellsworth, Wulfie Bain, Wyatt Thompson, Xiangning Chen, Xiangyu Qi, Xin Xiang, Xinwei Shi, Yann Dubois, Yaodong Yu, Yara Khakbaz, Yifan Wu, Yilei Qian, Yin Tat Lee, Yinbo Chen, Yizhen Zhang, Yizhong Xiong, Yonglong Tian, Young Cha, Yu Bai, Yu Yang, Yuan Yuan, Yuanzhi Li, Yufeng Zhang, Yuguang Yang, Yujia Jin, Yun Jiang, Yunyun Wang, Yushi Wang, Yutian Liu, Zach Stubenvoll, Zehao Dou, Zheng Wu, and Zhigang Wang. Openai gpt-5 system card, 2025. URL <https://arxiv.org/abs/2601.03267>.

- Adly Templeton, Tom Conerly, Jonathan Marcus, Jack Lindsey, Trenton Bricken, Brian Chen, Adam Pearce, Craig Citro, Emmanuel Ameisen, Andy Jones, Hoagy Cunningham, Nicholas L Turner, Callum McDougall, Monte MacDiarmid, C. Daniel Freeman, Theodore R. Sumers, Edward Rees, Joshua Batson, Adam Jermyn, Shan Carter, Chris Olah, and Tom Henighan. Scaling monosemanticity: Extracting interpretable features from claude 3 sonnet. *Transformer Circuits Thread*, 2024. URL <https://transformer-circuits.pub/2024/scaling-monosemanticity/index.html>.
- Curt Tigges, Oskar John Hollinsworth, Atticus Geiger, and Neel Nanda. Linear representations of sentiment in large language models. *CoRR*, abs/2310.15154, 2023. doi: 10.48550/ARXIV.2310.15154. URL <https://doi.org/10.48550/arXiv.2310.15154>.
- Denny Vrandečić and Markus Krötzsch. Wikidata: a free collaborative knowledgebase. *Commun. ACM*, 57(10):78–85, September 2014. ISSN 0001-0782. doi: 10.1145/2629489. URL <https://doi.org/10.1145/2629489>.
- An Yang, Anfeng Li, Baosong Yang, Beichen Zhang, Binyuan Hui, Bo Zheng, Bowen Yu, Chang Gao, Chengen Huang, Chenxu Lv, Chujie Zheng, Dayiheng Liu, Fan Zhou, Fei Huang, Feng Hu, Hao Ge, Haoran Wei, Huan Lin, Jialong Tang, Jian Yang, Jianhong Tu, Jianwei Zhang, Jianxin Yang, Jiayi Yang, Jing Zhou, Jingren Zhou, Junyang Lin, Kai Dang, Keqin Bao, Kexin Yang, Le Yu, Lianghao Deng, Mei Li, Mingfeng Xue, Mingze Li, Pei Zhang, Peng Wang, Qin Zhu, Rui Men, Ruize Gao, Shixuan Liu, Shuang Luo, Tianhao Li, Tianyi Tang, Wenbiao Yin, Xingzhang Ren, Xinyu Wang, Xinyu Zhang, Xuancheng Ren, Yang Fan, Yang Su, Yichang Zhang, Yinger Zhang, Yu Wan, Yuqiong Liu, Zekun Wang, Zeyu Cui, Zhenru Zhang, Zhipeng Zhou, and Zihan Qiu. Qwen3 technical report, 2025. URL <https://arxiv.org/abs/2505.09388>.
- Xiang Zhang, Junbo Jake Zhao, and Yann LeCun. Character-level convolutional networks for text classification. In Corinna Cortes, Neil D. Lawrence, Daniel D. Lee, Masashi Sugiyama, and Roman Garnett (eds.), *Advances in Neural Information Processing Systems 28: Annual Conference on Neural Information Processing Systems 2015, December 7-12, 2015, Montreal, Quebec, Canada*, pp. 649–657, 2015. URL <https://proceedings.neurips.cc/paper/2015/hash/250cf8b51c773f3f8dc8b4be867a9a02-Abstract.html>.
- Andy Zou, Long Phan, Sarah Chen, James Campbell, Phillip Guo, Richard Ren, Alexander Pan, Xuwang Yin, Mantas Mazeika, Ann-Kathrin Dombrowski, et al. Representation engineering: A top-down approach to ai transparency, 2023. URL <https://arxiv.org/abs/2310.01405>, 97, 2023.

Depth	Locations	Research Topic	Persons	Organizations	Organisms
<b>Model: Llama 3.2 3B</b>					
0 (Root)	1	1	1	1	1
1	5	3	6	5	6
2	21	12	31	14	40
3	151	79	188	157	354
4	20820	1302	–	–	–
<b>Model: Llama 3.1 8B</b>					
0 (Root)	1	1	1	1	1
1	5	4	6	6	6
2	22	19	33	18	48
3	168	140	202	196	389
4	25037	1959	–	–	–
<b>Model: Qwen3 8B</b>					
0 (Root)	1	1	1	1	1
1	5	4	6	6	6
2	22	17	33	18	48
3	168	132	202	196	387
4	21891	1800	–	–	–
<b>Model: Qwen3 14B</b>					
0 (Root)	1	1	1	1	1
1	5	4	6	5	6
2	22	19	34	16	46
3	169	143	205	182	385
4	22416	1913	–	–	–

Table 6: Number of LM-filtered examples by hierarchical depth across domains and models, where parent-child relations are retained only when the model correctly predicts the parent category

## A Details of the Data

In this study, we use hierarchical datasets from five domains: Locations, Persons, Organizations, Organisms, and Research Topics. For the location domain, we use the ISO 3166-1 country code dataset, which includes country classifications based on the United Nations geoscheme (Duncalfe, 2024), together with the geographic data used by Gurnee & Tegmark (2024). For the person and organization domains, we first generated candidate entities using GPT-5 (Singh et al., 2025) and then filtered them to retain only entries that exist in Wikidata (Vrandečić & Krötzsch, 2014), thereby ensuring that the entities correspond to real-world instances. We chose to use GPT-5 for candidate generation because knowledge bases such as Wikidata sometimes contain category names introduced primarily for taxonomic convenience, including expressions that are not commonly used in the real world. For the organism domain, we use the dataset of Park et al. (2025) and organize it according to the Linnaean taxonomic hierarchy. For the research topic domain, we use publicly available data from OpenAlex (Barrett, 2024). Concrete examples of the hierarchical data are shown in Fig. 9.

We then filtered the data to retain only those instances that each model answered correctly in a few-shot multiple-choice question answering setting. The resulting number of filtered instances for each model is reported in Tbl. 6. The prompt used for this filtering step is shown in Fig. 10. We used five few-shot examples during filtering.

## B Details of the Training Setup

For training the linear transformations, we used eight training samples for each linear transformation, following the setup of LRC (Chanin et al., 2024). The training samples were

Models	Hidden dim.	#Layer	#Head
Llama 3.2 3B	3072	28	24
Llama 3.1 8B	4096	32	32
Qwen3 8B	4096	36	32
Qwen3 14B	5120	40	40

Table 7: Hyperparameters of each model’s architecture.

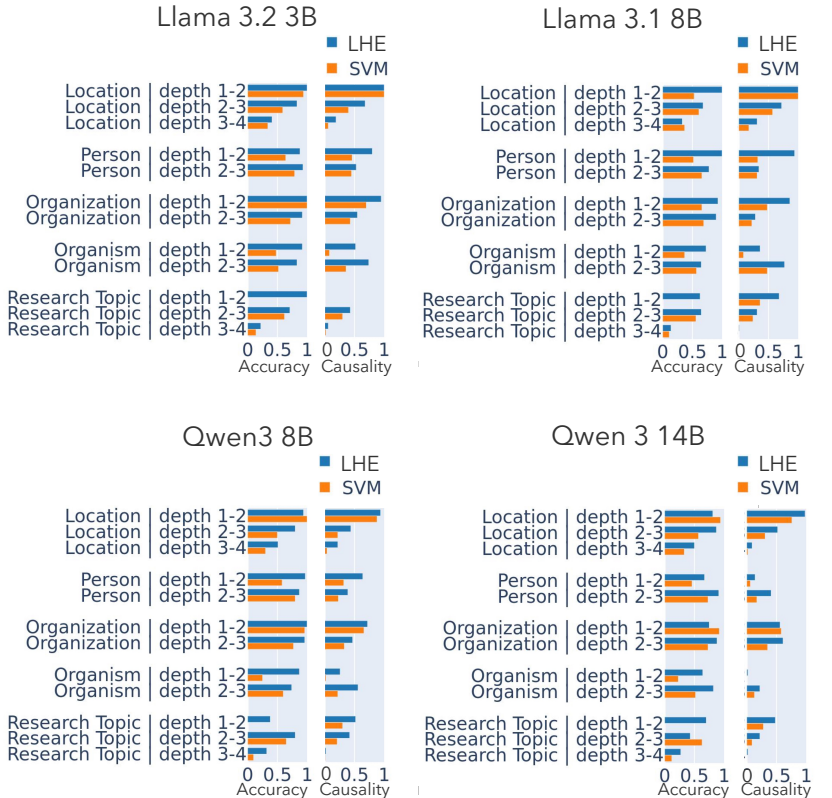


Figure 8: Accuracy and Causality at each hierarchy depth for all models. The Accuracy reported in this figure is chance-corrected to account for the depth-specific chance rate and to enable fair comparison across depths.

drawn using five different random seeds, and all reported results are averaged over these seeds. For each sample, we used a few-shot prompt with five in-context examples. We used the same prompt format at evaluation time.

### C Hyperparameters for Each Model Used in the Experiments

Tbl. 8 summarizes the hyperparameters used for LRC training and inference for each model. These values were selected through a grid search based on the best average score of Accuracy and Causality. The selected hyperparameters were obtained from the sweep described in App. E.

### D Results for All Models

Tbl. 10 reports the Accuracy and Causality results for all models. In addition, Tbl. 11 presents the results obtained using prompt variants with different template formats, shown

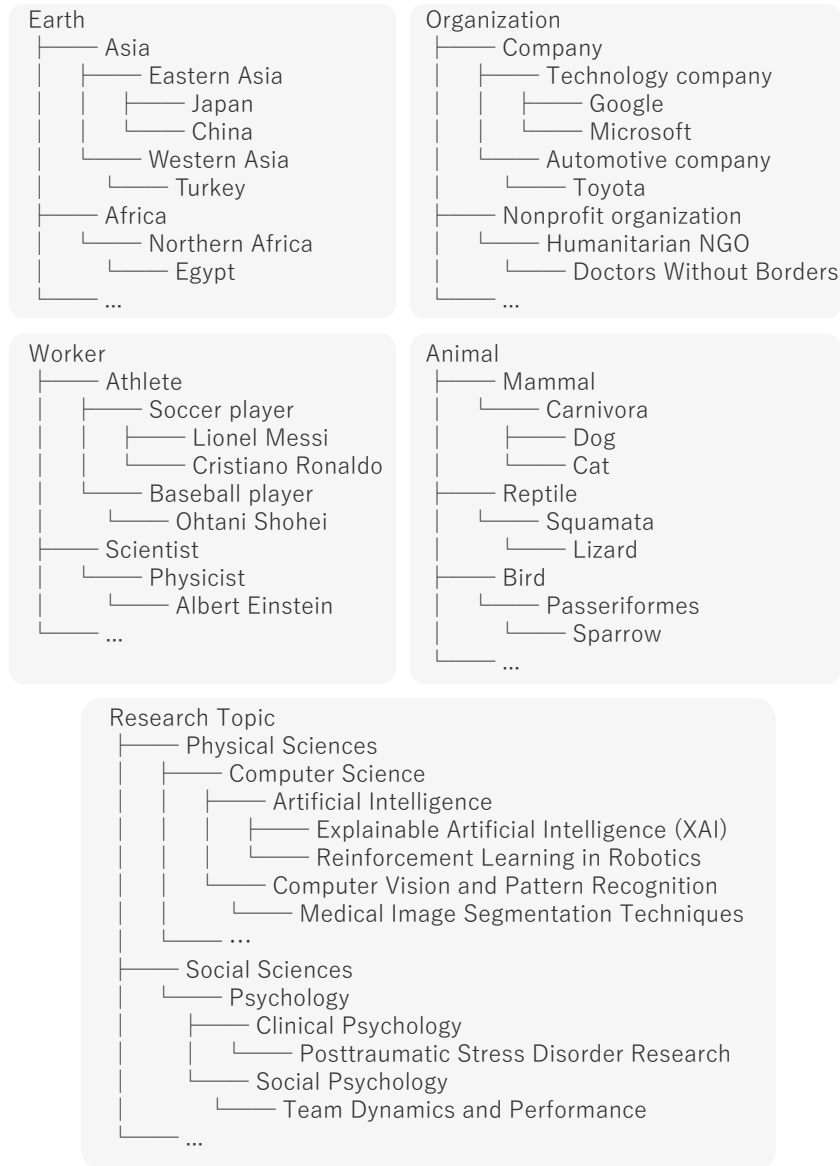


Figure 9: Examples of data representing the hierarchical structure of concepts.

Model	Subject Layer	Object Layer	Rank
Llama 3.2 3B	12	15	128
Llama 3.1 8B	12	21	160
Qwen3 8B Base	20	27	192
Qwen3 14B Base	25	28	256

Table 8: Hyperparameters used for LRC training and inference for each model.

in Fig. 11. Fig. 12 shows the results of the cross-domain evaluation for all models. Fig. 16 shows the subspace similarity results for all models.

---

Task: Pick the best higher-level label (parent concept) for the given Item from the options.

Rules: Output ONLY the chosen label text exactly as written in the options.

Example 1:

Item: {child node name}

Options:

- {parent concept 1}

- {parent concept 2}

- {parent concept 3}

- {parent concept 4}

Answer: {correct parent concept}

...(omitted)...

Example 5:

Item: {child node name}

Options:

- {parent concept 1}

- {parent concept 2}

- {parent concept 3}

- {parent concept 4}

- {parent concept 5}

Answer: {correct parent concept}

Now answer:

Item: {test child node name}

Options:

- {option 1}

- {option 2}

- {option 3}

- {option 4}

- {option 5}

Answer:

---

Figure 10: Prompt format used for both data filtering and the main experiments.

## E Results of the Hyperparameter Sweep

In this section, we report how the scores vary when sweeping the effective rank of the linear transformation, as well as the choices of the subject layer and object layer. Fig. 13 shows the results of sweeping the rank. Fig. 14 shows the results of sweeping the subject layer. Fig. 15 shows the results of sweeping the object layer.

## F PCA Visualizations

Fig. 17 shows PCA visualizations of the concept vectors obtained from the other domains. The model used in this analysis is Llama 3.1 8B.

## G Experimental Details for the Topological Data Analysis

In our experiments, for each domain we treat the set of concept vectors as a point cloud, compute persistent homology under Euclidean distance, and obtain a persistence diagram.

{child node name 1} is a {parent node name 1} {child node name 2} is a {parent node name 2} {child node name 3} is a {parent node name 3} {child node name 4} is a {parent node name 4} {child node name 5} is a {parent node name 5} {test child node name} is a
{child node name 1} is part of {parent node name 1} {child node name 2} is part of {parent node name 2} {child node name 3} is part of {parent node name 3} {child node name 4} is part of {parent node name 4} {child node name 5} is part of {parent node name 5} {test child node name} is part of

Figure 11: Few-shot prompts in the template-based format. The is-a template is used for the Person, Organization, Organism, and Research Topic domains, whereas the part-of template is used for the Location domain. Results obtained with these prompts are shown in Tbl. 11.

<b>[Organism] panther</b> Pred: panther $\subset$ <span style="background-color: #e0ffe0;">Carnivora</span> $\subset$ <span style="background-color: #e0ffe0;">Mammal</span> $\checkmark$ Gold: panther $\subset$ Carnivora $\subset$ Mammal	<b>All correct</b>
<b>[Organization] Toyota</b> Pred: Toyota $\subset$ <span style="background-color: #e0ffe0;">Automotive company</span> $\subset$ <span style="background-color: #e0ffe0;">Company</span> $\checkmark$ Gold: Toyota $\subset$ Automotive company $\subset$ Company	<b>All correct</b>
<b>[Research Topic] Information Retrieval and Search Behavior</b> Pred: Information Retrieval and Search Behavior $\subset$ <span style="background-color: #e0ffe0;">Information Systems</span> $\subset$ <span style="background-color: #e0ffe0;">Computer Science</span> $\checkmark$ $\not\subset$ <span style="background-color: #ffe0e0;">Social Sciences</span> $\times$ Gold: Information Retrieval and Search Behavior $\subset$ Information Systems $\subset$ Computer Science $\subset$ Physical Sciences	<b>Bottom <math>\checkmark</math>, Top <math>\times</math></b>

Table 9: Qualitative examples for accuracy using Llama 3.1 8B. Each row shows an entity and its predicted parent chain (**Pred**) with step-wise correctness ( $\checkmark$ / $\times$ ) against the gold chain (**Gold**). Correct and incorrect predicted parents are highlighted in green and red, respectively, and  $\subset$  /  $\not\subset$  indicate inclusion vs. non-inclusion relations between consecutive depths. We group cases by whether errors occur earlier vs. later along the evaluated depth sequence; this table shows representative instances of *All correct*, *Bottom  $\times$* , *Top  $\checkmark$* , and *Bottom  $\checkmark$ , Top  $\times$* .

We then quantify cross-domain similarity by computing the Wasserstein distance between persistence diagrams. Intuitively, a persistence diagram summarizes how topological features of the point cloud (e.g., mergers of connected components, formation of loops) *appear* (birth) and *disappear* (death) as we gradually increase the radius  $\epsilon$  of balls centered at each point; it represents these events as a multiset of birth–death pairs. Smaller distances between diagrams indicate more similar representational structure across domains. The results for all models obtained in these experiments are shown in Fig. 18.

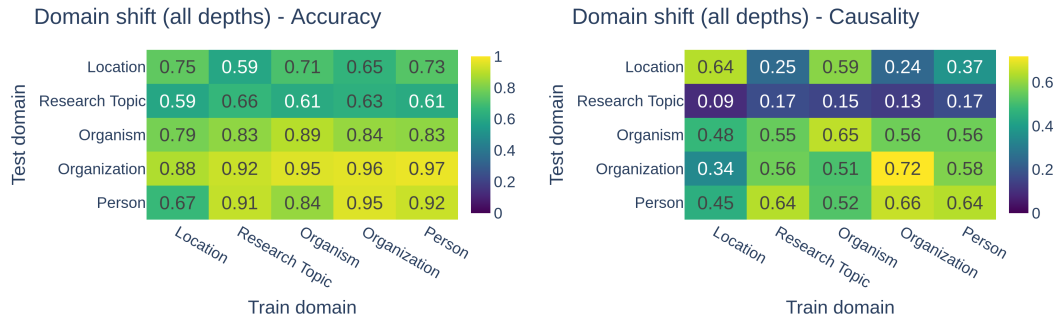
<b>Llama 3.2 3B</b>					
<b>Accuracy</b>					
Method	Locations	Research Topic	Persons	Organizations	Organisms
Input averaging	0.47	0.36	0.60	0.63	0.48
SVM	0.64	0.37	0.75	0.87	0.56
LHE	<b>0.75</b>	<b>0.66</b>	<b>0.92</b>	<b>0.96</b>	<b>0.89</b>
<b>Causality</b>					
Method	Locations	Research Topic	Persons	Organizations	Organisms
Input averaging	0.43	0.07	0.24	0.10	0.16
SVM	0.49	0.11	0.46	0.56	0.22
LHE	<b>0.62</b>	<b>0.17</b>	<b>0.67</b>	<b>0.75</b>	<b>0.63</b>
<b>Llama 3.1 8B</b>					
<b>Accuracy</b>					
Method	Locations	Research Topic	Persons	Organizations	Organisms
Input averaging	0.41	0.29	0.47	0.35	0.44
SVM	0.55	0.36	0.63	0.72	0.55
LHE	<b>0.68</b>	<b>0.52</b>	<b>0.89</b>	<b>0.93</b>	<b>0.72</b>
<b>Causality</b>					
Method	Locations	Research Topic	Persons	Organizations	Organisms
Input averaging	0.42	0.05	0.10	0.07	0.18
SVM	0.58	0.20	0.32	0.35	0.28
LHE	<b>0.67</b>	<b>0.35</b>	<b>0.65</b>	<b>0.57</b>	<b>0.57</b>
<b>Qwen3 8B</b>					
<b>Accuracy</b>					
Method	Locations	Research Topic	Persons	Organizations	Organisms
Input averaging	0.55	0.28	0.69	0.81	0.44
SVM	0.61	0.31	0.73	0.88	0.50
LHE	<b>0.76</b>	<b>0.56</b>	<b>0.93</b>	<b>0.98</b>	<b>0.82</b>
<b>Causality</b>					
Method	Locations	Research Topic	Persons	Organizations	Organisms
Input averaging	0.41	0.12	0.15	0.33	0.19
SVM	0.38	0.17	0.28	0.49	0.12
LHE	<b>0.53</b>	<b>0.32</b>	<b>0.51</b>	<b>0.60</b>	<b>0.41</b>
<b>Qwen3 14B</b>					
<b>Accuracy</b>					
Method	Locations	Research Topic	Persons	Organizations	Organisms
Input averaging	0.47	0.29	0.58	0.56	0.42
SVM	0.63	0.32	0.65	0.84	0.45
LHE	<b>0.74</b>	<b>0.51</b>	<b>0.82</b>	<b>0.85</b>	<b>0.76</b>
<b>Causality</b>					
Method	Locations	Research Topic	Persons	Organizations	Organisms
Input averaging	<b>0.55</b>	0.17	0.19	0.50	<b>0.15</b>
SVM	0.36	0.13	0.11	0.46	0.07
LHE	0.53	<b>0.24</b>	<b>0.28</b>	<b>0.58</b>	0.12

Table 10: Accuracy and causality by domain for four LMs, evaluated using the prompt format shown in Figure 10. Scores are averaged across hierarchical levels.

Llama 3.2 3B					
Accuracy					
Method	Locations	Research Topic	Persons	Organizations	Organisms
Input averaging	0.44	0.35	0.62	0.80	0.47
SVM	0.58	0.35	0.70	0.91	0.52
LHE	<b>0.78</b>	<b>0.62</b>	<b>0.99</b>	<b>0.95</b>	<b>0.81</b>
Causality					
Method	Locations	Research Topic	Persons	Organizations	Organisms
Input averaging	0.74	0.25	0.52	0.62	0.47
SVM	0.76	0.28	0.73	0.74	0.51
LHE	<b>0.83</b>	<b>0.34</b>	<b>0.82</b>	<b>0.87</b>	<b>0.72</b>
Llama 3.1 8B					
Accuracy					
Method	Locations	Research Topic	Persons	Organizations	Organisms
Input averaging	0.48	0.39	0.59	0.64	0.53
SVM	0.61	0.42	0.65	0.79	0.57
LHE	<b>0.71</b>	<b>0.59</b>	<b>0.88</b>	<b>0.98</b>	<b>0.78</b>
Causality					
Method	Locations	Research Topic	Persons	Organizations	Organisms
Input averaging	0.72	0.24	0.70	0.54	0.55
SVM	0.73	0.33	0.82	0.72	0.56
LHE	<b>0.84</b>	<b>0.57</b>	<b>0.92</b>	<b>0.87</b>	<b>0.80</b>
Qwen3 8B					
Accuracy					
Method	Locations	Research Topic	Persons	Organizations	Organisms
Input averaging	0.44	0.27	0.59	0.66	0.57
SVM	0.58	0.32	0.64	0.87	0.57
LHE	<b>0.78</b>	<b>0.62</b>	<b>0.95</b>	<b>0.98</b>	<b>0.79</b>
Causality					
Method	Locations	Research Topic	Persons	Organizations	Organisms
Input averaging	0.78	0.30	0.67	0.48	0.46
SVM	0.57	0.13	0.25	0.53	0.34
LHE	<b>0.80</b>	<b>0.60</b>	<b>0.77</b>	<b>0.79</b>	<b>0.63</b>
Qwen3 14B					
Accuracy					
Method	Locations	Research Topic	Persons	Organizations	Organisms
Input averaging	0.43	0.34	0.45	0.65	0.48
SVM	0.63	0.39	0.61	0.87	0.52
LHE	<b>0.84</b>	<b>0.61</b>	<b>0.98</b>	<b>0.98</b>	<b>0.80</b>
Causality					
Method	Locations	Research Topic	Persons	Organizations	Organisms
Input averaging	<b>0.79</b>	0.28	0.68	0.55	<b>0.54</b>
SVM	0.45	0.09	0.25	0.45	0.32
LHE	0.71	<b>0.38</b>	<b>0.78</b>	<b>0.75</b>	0.47

Table 11: Accuracy and causality by domain for four LMs, evaluated using the prompt format shown in Figure 11. Scores are averaged across hierarchical levels.

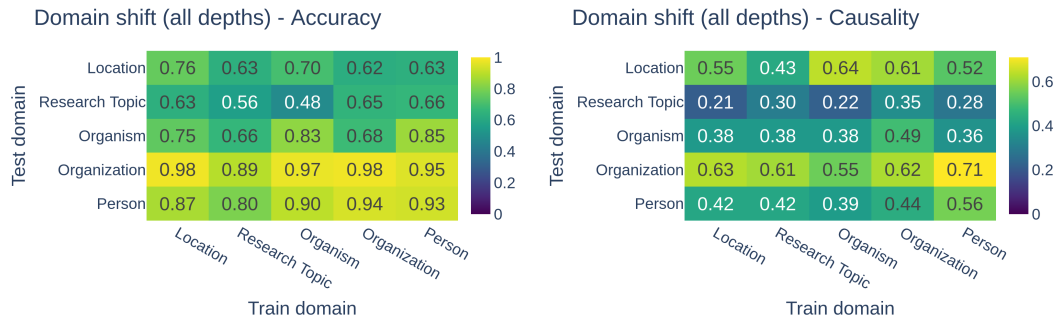
### Llama 3.2 3B



### Llama 3.1 8B



### Qwen3 8B



### Qwen 3 14B

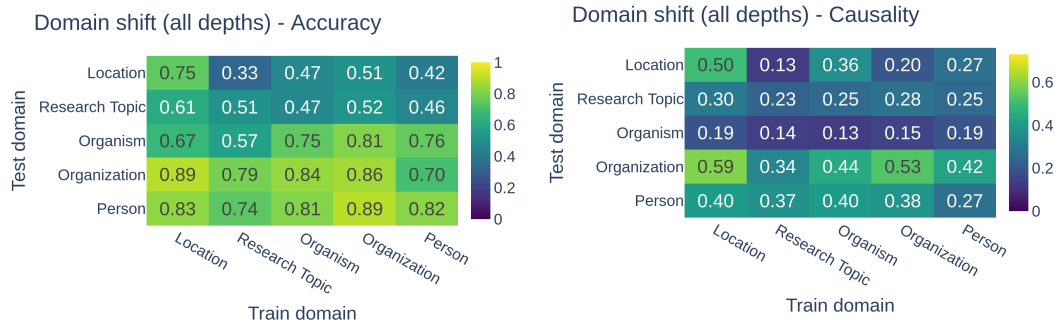


Figure 12: Cross-domain evaluation of hierarchical-structure directions for all models.

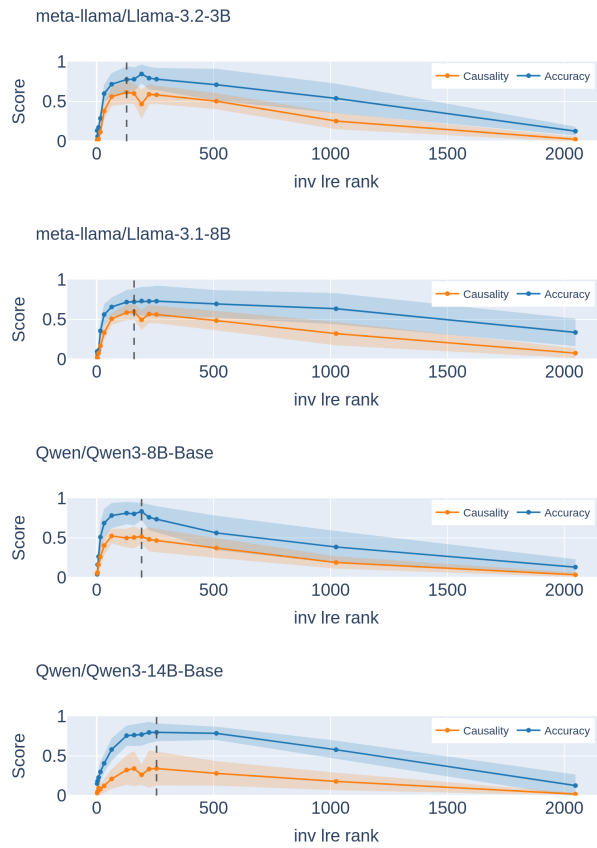


Figure 13: Results of sweeping the rank of the pseudo-inverse matrix  $\mathbf{W}_r^+$  for all models. Scores are averaged across all domains. The vertical dotted line indicates the point at which the average of Accuracy and Causality is maximized.

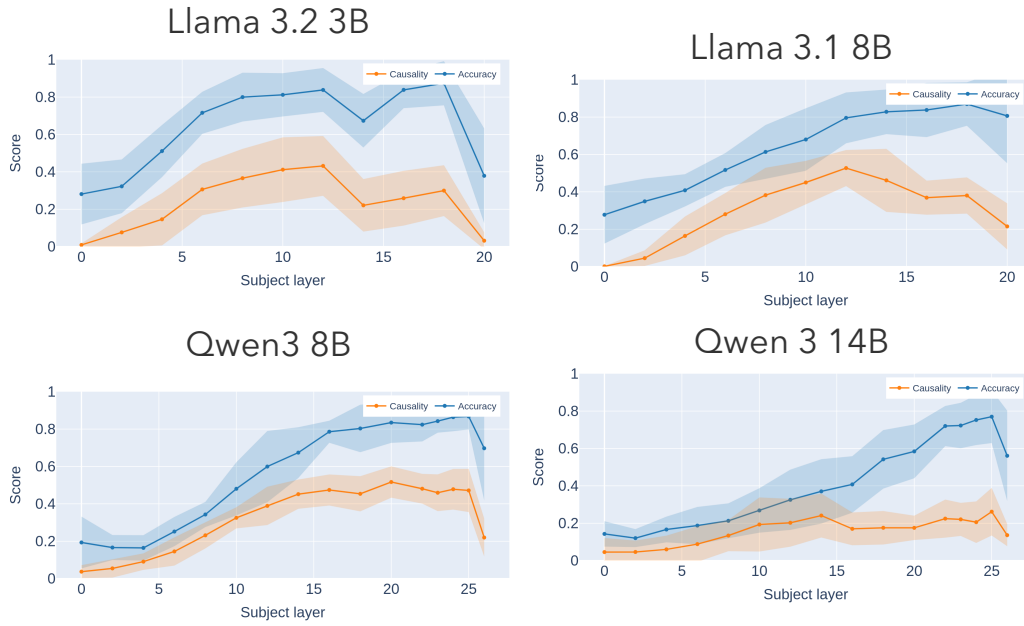


Figure 14: Accuracy and Causality obtained by sweeping the subject layer while keeping the object layer fixed.

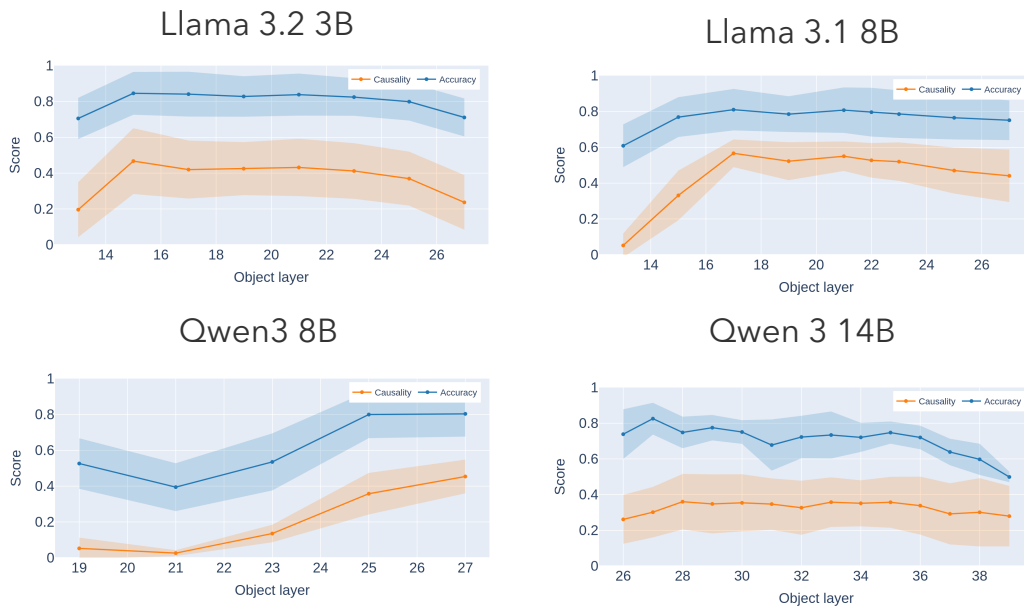


Figure 15: Accuracy and Causality obtained by sweeping the object layer while keeping the subject layer fixed.

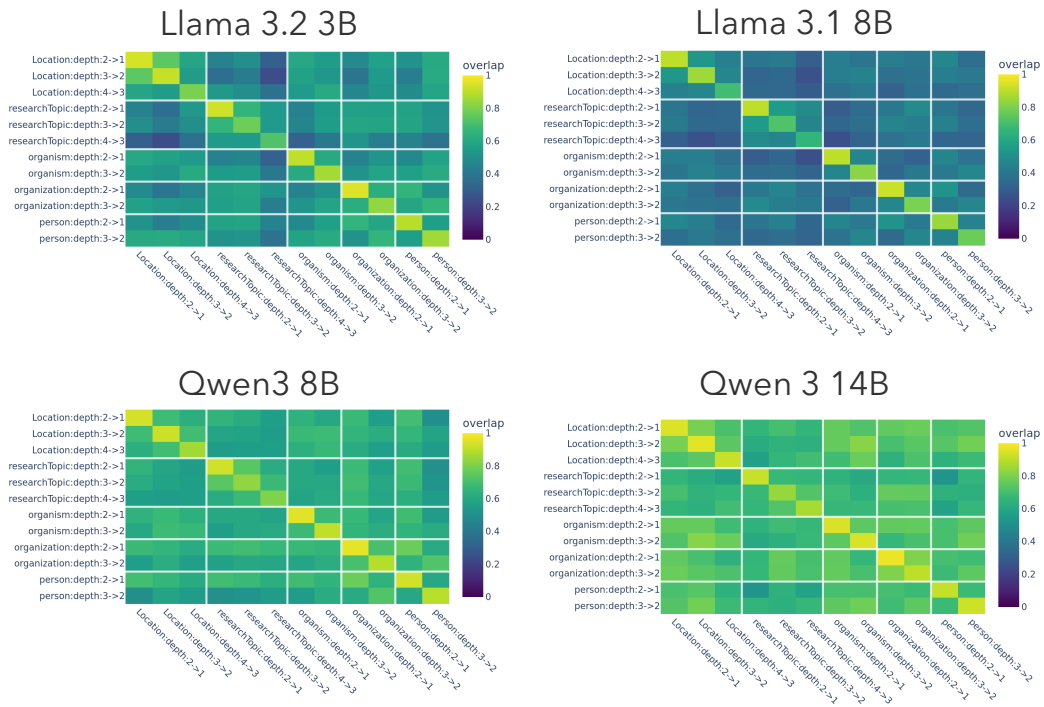


Figure 16: Subspace similarity of subject representations for all models.

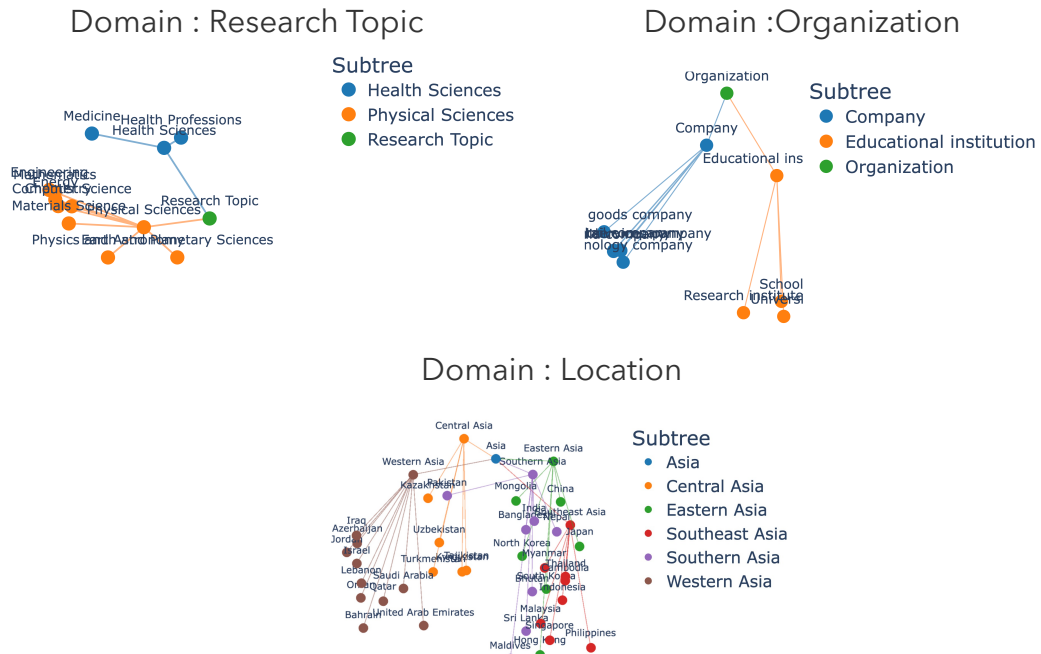


Figure 17: PCA visualizations of the concept vectors for Llama 3.1 8B.

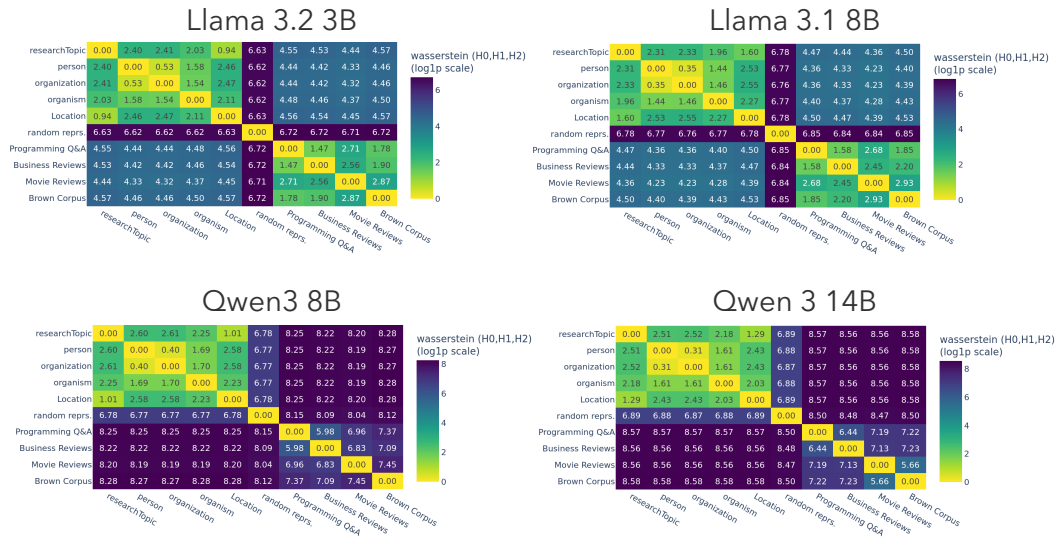


Figure 18: Similarity matrices of LM representations for all models, based on persistent homology. Each entry shows the Wasserstein distance (computed on persistence diagrams derived from the concept vector point clouds; log<sub>1p</sub> scale) between a pair of domains/-datasets. Smaller values indicate more similar representational structure.